A first experiment of 3D imaging with a ground based parasitic SAR

C. Colesanti
formerly with Dip. di Elettronica e Informazione,
Politecnico di Milano,
Milano, Italy

D. Perissin
Dip. di Elettronica e Informazione,
Politecnico di Milano,
Milano, Italy
perissin@elet.polimi.it

***Abstract*— The present paper provides the first example of 3D imaging using the ground based parasitic SAR instrument developed in the past years at Politecnico di Milano.**

Keywords: 3D SAR imaging, ground based parasitic SAR, geostationary broadcasting satellite.

I. INTRODUCTION

In the past years the SAR research group of Politecnico di Milano has investigated the feasibility of a parasitic SAR system reusing the signal transmitted by nominally geostationary broadcasting satellites. The original idea was to equip the very same (or a different) satellite with a receiving antenna so as to gather the signal scattered back from the Earth surface [1], [2] and [3]. Later, in order to render preliminary experiments more easily feasible, a ground based receiver has also been designed. This lead to a bistatic SAR system where:

- The signal source is a nominally geostationary TV broadcasting satellite;
- The non-ideality of the geostationary orbit of the satellite (in particular the non-null inclination with respect to the equatorial plane and the non-null eccentricity) make the satellite move along a daily track that, seen from a point on the Earth surface, corresponds to an ellipse with axes in the order of 50-80 km. This movement provides the synthetic aperture;
- A ground based receiving station gathers both the signal arriving directly from the satellite (as a reference signal) and the signal scattered from a target scene in the immediate neighborhood of the receiving station itself.

Both the theoretical framework (given the peculiar bistatic imaging geometry) and the first successful experiments (focused images) are reported in [4] and [5]. The problem of estimating the (a priory unknown) satellite's orbit from the phase history of at least two scatterers in known positions is also addressed therein. Key advantages of the system are: (1) the very limited cost (a few thousands of US$), (2) the suitability for continuous monitoring since the area to be imaged is illuminated 24 hours a day. On the other hand the main limiting factor is a very critical link power budget. An initially dramatically low SNR is heavily improved by range and azimuth focusing operations that correspond to a (coherent) averaging process continued for 24 hours (the orbit period). Ad hoc deployed and oriented metallic scatterers proofed being well visible (at least at distances of several hundreds of meters). It is, however, not yet clear to which extent natural targets provide a reasonable SNR in focused images.

II. 3D IMAGING

Given that the orbit of the source satellite (as seen from the ground) extends along two dimensions, three-dimensional imaging is feasible, in analogy to what is achievable via circular SAR [6].

Due to the very particular bistatic geometry of the ground based parasitic SAR, it is worthwhile investigating briefly the 3D imaging capabilities of the system, in particular providing the equations of iso-range and iso-azimuth surfaces, thereby highlighting the range and azimuth resolution and giving some insights on the impulse response along range and azimuth.

To this end we will refer to the imaging geometry sketched in Figure 1. The reference system is centered at the ground based receiving station, the x axis points towards East and the y axis towards North. The position of the satellite is identified by the pair (θ,ϕ). The generic target P to be imaged is in position (x_s,y_s,z_s).

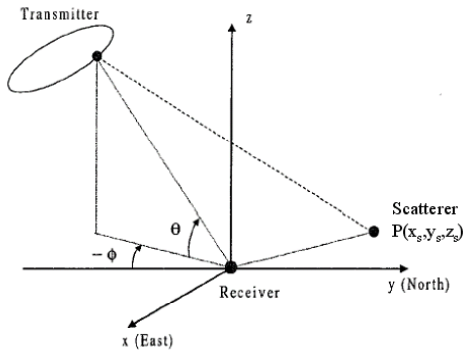

Figure 1. Imaging geometry of the ground based parasitic SAR system.

A. Range

Range focusing is performed via the cross-correlation of the reference signal arriving directly from the satellite and the signal scattered back towards the ground based receiving station. The source signal corresponds usually to a digital TV channel (bandwidth $B \approx 20$ MHz), that is transmitted in compressed format (e.g. MPEG), thereby resulting in a band-limited white sequence. The cross-correlation is, therefore, impulsive. Due to the spectral shaping effect of the cascade of filters used at the transmitter and at the receiver, the main lobe of the cross-correlation $R(\tau)$ turned (experimentally) out being well approximated by a squared cardinal sine [7], whose first zero is at $\tau_0 = 2/B$. This represents the system impulse response in range direction.

The cross-correlation peak allows one to identify the travel path difference $\Delta r = c\tau$ (c: light speed in vacuum) between direct and scattered contribution and, therefore, the position of the scatterer along range:

$$\Delta r = \sqrt{x_s^2 + y_s^2 + z_s^2} - x_s \cos\theta \sin\phi + y_s \cos\theta \cos\phi + z_s \sin\theta \qquad (1)$$

An iso-range surface (i.e. the set of points to which the system would assign the very same range position) is, then, identified by the equation Δr=constant, which defines a 3D ellipsoid (in radio-propagation theory it is called Fresnel ellipsoid [4]). In order to be mutually resolvable, the points of two iso-range surfaces must be spaced along range by $\alpha c/B$ (α is a constant, with value approximately between 0.9 and 1.5). The family of the mutually resolvable iso-range surfaces can, then, be expressed as:

$$\sqrt{x_s^2 + y_s^2 + z_s^2} - x_s \cos\theta \sin\phi + y_s \cos\theta \cos\phi + z_s \sin\theta = m\frac{c}{B} \qquad (2)$$

where m is an arbitrary integer (it has been assumed, for the sake of simplicity, α=1). Typical values for the range resolution are in the order of 10-15m. Approaching the ground based station, i.e. the origin of the reference system, the range resolution capability decreases.

The family of the mutually resolvable iso-range surfaces is displayed in Figure 2. The plot refers to the scene imaged during the experiments carried out, see Section III.

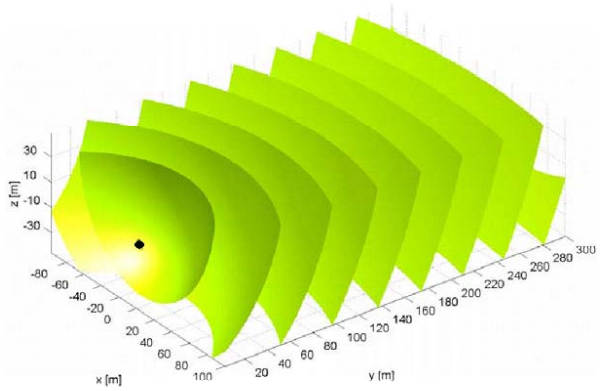

Figure 2. Iso-range surfaces. The origin of the reference system (i.e. the position of the receiving station) is marked by a black dot.

B. Azimuth

Given the limited size of ground based parasitic SAR images (in the experimental results shown here 200x300 m^2, in general up to a few tens of km^2), azimuth focusing is carried out easily in the time (or space) domain.

The phase history of a radar target P (i.e. the evolution of its phase while the satellite moves along its daily orbit) can be expressed starting from equation (1), taking into account that $\phi(t)$ and $\theta(t)$ are sinusoidal functions of time, with a period T corresponding to 1 day [8], [4]:

$$\theta(t) = \theta_0 + A_\theta \sin\left(\frac{2\pi}{T}t + \theta_{ini}\right) \qquad (3)$$

$$\phi(t) = \phi_0 + A_\phi \sin\left(\frac{2\pi}{T}t + \phi_{ini}\right) \qquad (4)$$

Since $A_\phi << \phi_0$ and $A_\theta << \theta_0$, the expressions of $\phi(t)$ and $\theta(t)$ can be approximated very effectively using a first order Taylor expansion centered around (ϕ_0, θ_0). Omitting constant terms, following expression holds:

$$\psi_P(t) = \frac{2\pi}{\lambda}(\phi(t) - \phi_0)\cdot\left[-x_s \cos\theta_0 \cos\phi_0 - y_s \cos\theta_0 \sin\phi_0\right] + \qquad (5)$$

$$\frac{2\pi}{\lambda}(\theta(t) - \theta_0)\cdot\left[-x_s \sin\theta_0 \sin\phi_0 - y_s \sin\theta_0 \cos\phi_0 - z_s \cos\theta_0\right]$$

Setting:

$$K_1(x_s, y_s) = -x_s \cos\theta_0 \cos\phi_0 - y_s \cos\theta_0 \sin\phi_0 \qquad (6)$$

$$K_2(x_s, y_s, z_s) = x_s \sin\theta_0 \sin\phi_0 - y_s \sin\theta_0 \cos\phi_0 - z_s \cos\theta_0 \qquad (7)$$

and taking into account equations (3) and (4), equation (5) is clearly recognizable as the sum of two sinusoidal terms with the same period T=1 day. Therefore, $\psi_P(t)$ is itself sinusoidal:

$$\psi_P(t) = \frac{2\pi}{\lambda} A_\psi \cos\left(\frac{2\pi}{T}t + \psi_0\right) \qquad (8)$$

with amplitude A_ψ and initial phase ψ_0:

$$A_\psi = \sqrt{(K_1 A_\phi)^2 + (K_2 A_\theta)^2 + 2K_1 K_2 A_\phi A_\theta \cos(\phi_{ini} - \theta_{ini})} \qquad (9)$$

$$\psi_0 = \arctan\frac{K_1 A_\phi \sin\phi_{ini} + K_2 A_\theta \sin\theta_{ini}}{K_1 A_\phi \cos\phi_{ini} + K_2 A_\theta \cos\theta_{ini}} \qquad (10)$$

Azimuth focusing is carried out extracting (via interpolation) from the complex matrix of the range compressed data (in base-band representation) the contributions at $\tau_P = \tau_P(t, x_s, y_s, z_s)$, thereby getting the measured (amplitude and) phase history of the scatterer P: $A_P(t)\cdot\exp(j\,\psi_{P,mes}(t))$. The terms are compensated for the theoretical phase history $\psi_P(t)$ (see equations 5 and 8) and summed coherently getting the complex value to be assigned to the focused image in correspondence of the scatterer P:

$$\mathrm{Im}(P) = \mathrm{Im}(x_s, y_s, z_s) = \int_0^T A_P \cdot \exp j\left[\psi_{P,mes}(t) - \psi_P(t)\right] dt \qquad (11)$$

where $A_P(t)$ can be considered as constant (for non-decorrelating targets). As highlighted by equation (11), it is worthwhile remarking that, for generating a single image exploiting the whole synthetic aperture, the coherent summing operation extends over a full day. This implies that targets

losing coherence in less than a day are canceled out during azimuth focusing and will not even appear in the output SAR image [3].

Equation (11) provides also the basis for evaluating the azimuth impulse response and the azimuth resolution of the system. To this end, let us imagine to deal with a scene consisting in a single scatterer deployed in the origin of the coordinate system. Let us evaluate the term that (due to the presence of the scatterer in the origin) would be assigned to a pixel P' in a slightly different azimuth position. This corresponds to focusing (in position P') the contribution of the scatterer that is in the origin using the phase history expected for a scatterer in position P':

$$\mathrm{Im}(P') = \int_0^T A_P \cdot \exp\, j\left[\frac{2\pi}{\lambda} A_\psi(P') \cos\left(\frac{2\pi}{T} t + \psi_0(P')\right)\right] dt \qquad (12)$$

Remembering the identity [9]:

$$J_0(A) = \frac{1}{2\pi}\int_0^{2\pi} \exp\left[jA\cos\rho\right] d\rho \qquad (13)$$

where $J_0(A)$ is the zero order Bessel function of the first kind, we obtain:

$$\mathrm{Im}(P') \propto J_0\left(\frac{2\pi}{\lambda} A_\psi(P')\right) \qquad (14)$$

The azimuth impulse response of the ground based parasitic SAR is, therefore, proportional to $J_0(2\pi A_\psi(P')/\lambda)$, consistently with what already known for circular SAR systems [6].

Similarly, the first iso-azimuth surface (i.e. the set of points that the system is able to resolve in azimuth from an hypothetic scatterer deployed in the origin of the reference system) is characterized by the equation $A_\psi = \lambda\beta A_{null}/2\pi$ where β is a constant (e.g. in the order of 2) and $A_{null} \approx 2.4$ is the argument of the first zero of $J_0(A)$.

In practice, the mechanism allowing the system to resolve along the two azimuth directions is the varying dynamic range of the sinusoidal phase history of the scatterers (as a function of the coordinates of the scatterers themselves and of the satellite orbit). For the sake of simplicity it is convenient to set $\beta A_{null} = 2\pi$ which corresponds to assume that two scatterers can be solved in azimuth if the dynamic ranges of the respective phase histories differ by at least 2π. This leads to following expression for the family of the mutually resolvable iso-azimuth surfaces:

$$A_\psi = \sqrt{(K_1 A_\phi)^2 + (K_2 A_\theta)^2 + 2K_1 K_2 A_\phi A_\theta \cos(\phi_{ini} - \theta_{ini})} = m\lambda \qquad (9)$$

where m is an arbitrary integer. The equation represents a family of cylindroids with elliptical cross-section, whose axis is parallel to the direction identified by the pair (ϕ_0, θ_0) and goes through the origin of the reference system defined before. The increments of the two semi-axes of the elliptical cross-section between consecutive iso-azimuth surfaces identify the 2D azimuth resolution of the system. The two values of azimuth resolution depend on the shape and extension of the satellite's orbit, which in the long term (several months) can vary significantly [5]. Typical values range between 10 and 20m.

The family of the mutually resolvable iso-azimuth surfaces is displayed in Figure 3. The plot refers again to the scene imaged during the experiments carried out, see Section III.

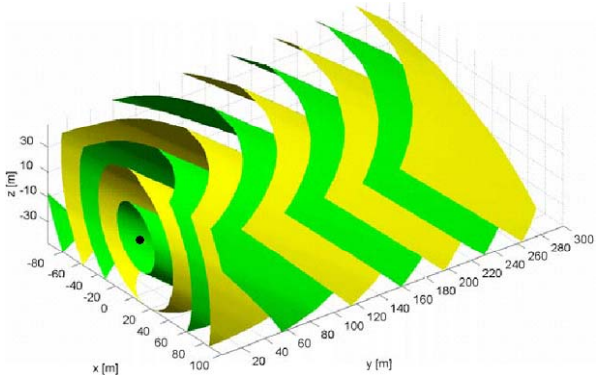

Figure 3. Iso-azimuth surfaces. The origin of the reference system (i.e. the position of the receiving station) is marked by a black dot.

III. Experimental Results

A. Setup

A measurement campaign has been carried out at the Joint Research Center (JRC) of the European Commission, in Ispra (Italy). The experimental setup used is an evolution of the one used in [4] and [5]. It was developed in the framework of [10]. In particular the digital oscilloscope was replaced by a third demodulation stage followed by a data acquisition board performing A/D conversion (AD40 by Innovative Integration). Furthermore, an ad hoc programmed processing board M67 (by Innovative Integration, mounting a TMS320C6701 DSP by Texas Instrument) carries out a real time range-focusing storing, finally, the matrix of range compressed data on the hard disk of a computer. In order to drive the data acquisition and processing a simple software interface has been developed using Labview (by National Instruments). 8 days and 8 hours data have been gathered in the time span from the 20th to the 28th of April 2001. The imaged scene contains three planar metallic scatterers (approximately 1x2 m^2) that were oriented so as to provide the maximal scattered signal at the ground based receiving station, which was hosted close to the top of a 15m tall wooden tower. The positions (x_s, y_s, z_s) of the scatterers are P_1=(0m, 35.1m, -12m), P_2=(-22.6m, 125m, -12m), P_3=(-20m, 225.1m, -12m). As in the experiments reported in [5], the signal transmitted by the satellite Hotbird 4 (by Eutelsat) has been used, in particular the signal corresponding to the TV channel at 10.9 GHz ($B \approx 20$ MHz).

B. *Results*

The expected (starting from orbital data provided by Eutelsat) and measured phase histories of the second scatterer are displayed in Figure 4. The residual (i.e. the difference) clearly shows a periodic behavior that turned out correlating pretty well with temperature records gathered in the very same days at a weather station several km away from the imaged scene [7]. The other scatterers show a very similar residual phase history. This provides a clear evidence of some thermal drift of one of the oscillators (very likely the one of the third demodulation stage). This, of course, turns out in a degradation of the focused image. In particular the scatterers are focused in a slightly displaced azimuth position, where the misplacement increases with the range coordinate of the scatterer (i.e. roughly speaking with the distance from the receiver). To compensate for this effect, the residual phase history of the 3rd scatterer was filtered, rescaled and used to compensate the residual phase histories of the first two scatterers [7].

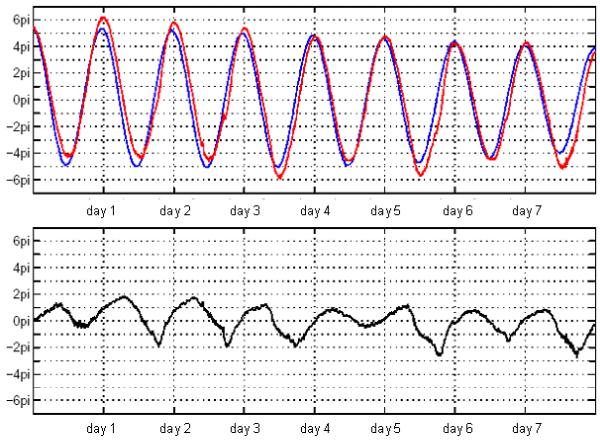

Figure 4. Above: Expected (blue) and measured (red) phase history of the scatterer P_2(-22.6m,125m,-12m). The expected phase history was evaluated starting from Hotbird 4 orbital data provided by Eutelsat. Below: difference between expected and measured phase histories.

This lead to focusing fully satisfactory 3D parasitic SAR images. Figure 5 displays the image obtained processing the data gathered on April, 21. The (pseudo-)cylindrical symmetry induced by the Bessel character of the azimuth impulse response is clearly visible. Similar results were obtained focusing the data relative to other days.

ACKNOWLEDGMENTS

The authors are grateful to Profs. F. Rocca and C. Prati that guided the whole research work carried out in the framework of the parasitic SAR project. Ing. M. Pandini programmed the acquisition and processing boards and performed the measurement campaign within an internship at the TDP unit, Space Application Institute (SAI), JRC. All members of the TDP unit, especially Dr. D. Tarchi and Dr. D. Leva, are also gratefully acknowledged. Ing. L. Tonini contributed to the generation of the focused 3D images. Eutelsat (Mr. G. Baraglia), provided the orbital data of Hotbird 4.

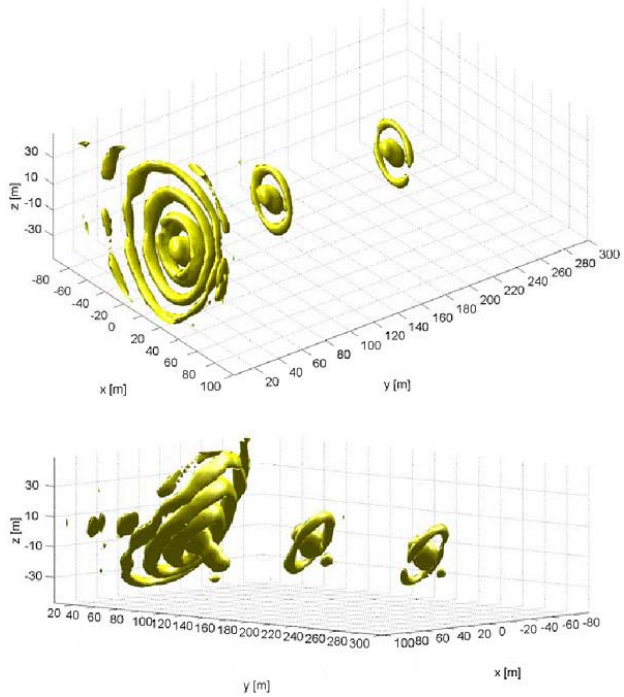

Figure 5. Focused 3D parasitic SAR image (seen from two different viewing angles) with the three planar metallic scatterers (SAR data of 21 April 2001).

REFERENCES

[1] M. Bonomelli and F. Porta, "Studio di un sistema SAR geostazionario passivo", Tesi di Laurea in Ing. Elettronica, Politecnico di Milano, Milano, Italy, 1994.

[2] D. Giancola and G. Quario, "Studio di fattibilità di un sistema SAR geostazionario", Tesi di Laurea Ing. Elettronica, Politecnico di Milano, Milano, Italy, 1995.

[3] C. Prati, F. Rocca, D. Giancola, and A. Monti Guarnieri, "Passive geosynchronous SAR system reusing backscattered digital audio broadcasting signals", IEEE Trans. Geosci. Remote Sensing, vol. 36, n. 6, pp. 1973–1976, Nov. 1998.

[4] C. Colesanti, L. Cazzani, "Esperimenti di SAR passivo con illuminatore quasi geostazionario e ricevitore a terra", Tesi di Laurea in Ing. delle Telecomunicazioni, Politecnico di Milano, Milano, Italy, 1999.

[5] L. Cazzani, C. Colesanti, D. Leva, G. Nesti, C. Prati, F. Rocca, D. Tarchi, "A ground based parasitic SAR experiment", IEEE Trans. Geosci. Remote Sensing, vol. 38, n. 5, pp. 2132-2141, Sept. 2000.

[6] A. Ishimaru, "An imaging technique using confocal circular synthetic aperture radar", IEEE Trans. Geosci. Remote Sensing, vol. 36, n. 5, pp. 1524-1530, Sept. 1998.

[7] D. Perissin, L. Tonini, "Focalizzazione tridimensionale di dati SAR da satellite geosincrono", Tesi di Laurea in Ing. delle Telecomunicazioni, Politecnico di Milano, Milano, Italy, 2002.

[8] E. M. Soop, "Introduction to geostationary orbits", ESA Scientific & Technical Publications Branch, Noordwijk, The Netherlands, SP-1053, 1983.

[9] M. Abramowitz, C. A. Stegun, Editors, "Modified Bessel functions I and K", chapter 9.6 in "Handbook of Mathematical Functions with Formulas, Graphs, and Mathematical Tables", 9th Reprint, New York, US, Dover, UK, 1972.

[10] M. Pandini, "Realizzazione e sperimentazione di un sistema SAR parassitico", Tesi di Laurea in Ing. delle Telecomunicazioni, Politecnico di Milano, Milano, Italy, 2001.